https://doi.org/10.5194/hess-2022-100
Preprint. Discussion started: 31 March 2022

Hydrology and Earth System Sciences
Discussions

Transit Time index (TTi) as an adaptation of humification index to illustrate transit time differences in karst hydrosystems. Application to the karst springs of Fontaine de Vaucluse system (Southeastern France)

Leïla Serène[1], Christelle Batiot-Guilhe[1], Naomi Mazzilli[2], Christophe Emblanch[2], Milanka Babic[2], Julien Dupont[2], Roland Simler[2], Matthieu Blanc[3], Gérard Massonnat[4]
[1]HSM, Univ. Montpellier, CNRS, IMT, IRD, Montpellier, France
[2]UMR 1114 EMMAH (AU-INRAE), Université d'Avignon, 84000 Avignon, France
[3]Independent researcher, Montpellier, France
[4]TotalEnergies, CSTJF, Avenue Larribau, CEDEX 64018 Pau, France

Correspondence to: Leïla Serène (leila.serene@umontpellier.fr)

Abstract. Transit time can be estimated thanks to natural tracers but few of them are usable in the 0-6 months range. The main purpose of this work is to analyze the potential of the ratio of heavy to light-weight organic compounds (HIX, Ohno, 2002; Zsolnay et al., 1999) as a natural tracer of short transit time (Blondel et al., 2012). Critical analysis of former studies shows that although the link between HIX and transit time seems consistent, the whole methodological approach needs to be consolidated. Natural organic matter fluorescence from 289 water samples from 4 springs and 10 flow points located in the unsaturated zone of the Vaucluse karst system is characterized by parallel factor analysis (PARAFAC) thanks to excitation-emission matrix (EEM), thus (i) allowing the identification of main fluorescent compounds of sampled groundwater; and (ii) evidencing the inadequacy of HIX 2D emission windows to characterize groundwater organic matter. We then propose a new humification index called Transit Time index (TTi) based on Ohno (2002) formula but using PARAFAC components of heavy and light organic matter from our samples instead of 2D windows. Finally, we evaluate TTi relevance as a transit time tracer by: (i) performing a detailed analysis of its dynamics on a selected spring (Millet) and (ii) comparing its mean value over karst springs of Fontaine de Vaucluse system. Principal component analysis (PCA) of TTi and other hydrochemical parameters monitored at Millet put in relief the different ranges of transit time associated with the different organic matter compounds. PCA results also provide evidence that TTi can detect a small proportion of fast infiltration water within a mix, while other natural tracers of transit time provide no or less sensitive information. TTi distributions at monitored karst springs are consistent with relative transit times expected for the small-scale, short average transit times systems. TTi thus appears as a relevant tracer of transit time in the 0-6 months range where existing tracers fail, even if the information on transit time is only qualitative at this stage.

https://doi.org/10.5194/hess-2022-100
Preprint. Discussion started: 31 March 2022

Hydrology and Earth System Sciences
Discussions

1 Introduction

Karst aquifers are essential for water supply at both global and local scales as they provide 9,2% of the world's drinking water and contribute to 13% of the total global withdrawal of groundwater (Stevanović, 2019). But karsts are also really complex and compartmentalized systems which offer very different paths to the infiltrated water. The hierarchized network of karst conduits allows a fast transit of recharge which is very specific to karst systems (White, 2002) and makes it essential to develop natural tracers of transit on short time scales (< 6 months). Natural tracers of stored water include major elements contents, isotopes and dissolved gas (Malík et al., 2016; Musgrove et al., 2019; Pérotin et al., 2021; Zhang et al., 2021); but little of these tracers allow to characterize fast infiltration. Indeed, natural tracers of transit time of this range must, by definition, see their contents vary at this time scale. While variations in inorganic compounds are small on this time scale, living and organic components of water like bacteria, Total Organic Carbon (TOC) or natural organic matter fluorescence (Batiot et al., 2003; Lapworth et al., 2008; Mudarra et al., 2011; Pronk et al., 2009; Sorensen et al., 2020) are suited to this goal. Indeed, TOC represents the quantity of organic matter present in the water and its mineralisation (or degradation) is complete after 6 months (Batiot, 2002). Fluorescent organic matter is a small part of the total organic matter represented by TOC and will therefore also be completely degraded after a maximum of 6 months. Our study focuses on fluorescent organic matter and its relation with transit time through Humification IndeX (HIX) as initially proposed by Blondel et al. (2012).

The humification index (HIX) expresses the maturation level of organic matter. Humification refers to the gradual transition of organic matter to highly metabolized compounds (humin). HIX is thus defined as the ratio of humic to non-humic compounds. In a study which aimed at identifying DOM sources in soil and sediment waters, Zsolnay (1999) proposed a methodology to derive HIX from fluorescence measurements. He identified the excitation wavelength most representative of fluorescent organic matter in soil water (254 nm). Next, he identified emissions wavelengths corresponding to light (L from 300 to 345 nm) and heavy (H from 435 to 480 nm) organic matters in the emission spectra with the assumption that emission wavelengths of fluorescent molecules increase while molecules get more condensed (Ewald et al., 1988; Zsolnay et al., 1999). HIX was then defined by the ratio H/L of integral under the emission curve of 2D spectra at 254 nm of excitation wavelength. This way of calculating HIX is dependent on DOM concentration because of the inner-filtering effect (Ohno, 2002). Inner-filtering effect results from either the absorption of excitation light by fluorescent molecules before it gets to the monitored zone (primary inner-filtering effect), or the absorption of emission light coming from photons (secondary inner-filtering effect, Tucker et al., 1992). Making H/L ratio to calculate HIX permits correction from primary inner filtering effect which affects each wavelength equally. But the secondary inner filtering effect still needs to be corrected if different study sites are to be compared (Mobed et al., 1996). Ohno (2002) thus proposed another HIX formula that corrects from both inner filter effects, Eq. (1) :

$$HIX = \frac{\mathrm{H}}{L+H} \qquad (1)$$

A quantitative relation between HIX and transit time was proposed by Blondel et al. (2012) based on natural fluorescence monitoring of 4 flow points collected in the unsaturated zone of Fontaine de Vaucluse system (France) during two hydrological

https://doi.org/10.5194/hess-2022-100
Preprint. Discussion started: 31 March 2022


Hydrology and Earth System Sciences
Discussions

cycles (2006-2007 and 2007-2008). Careful examination of this work revealed several methodological weaknesses. Calculated HIX used Zsolnay's formula (Zsolnay, 1999) which lacks secondary inner-filtering effect correction and thus prevents comparison between study sites. Excitation wavelength was 260 nm instead of 254 nm as recommended by Zsolnay (1999). In any case, Zsolnay emissions windows were calibrated for soil water, it is thus possible that they may be unsuitable for groundwater. Relation between HIX and transit time was obtained by considering the mean Total Organic Carbon (TOC) value for each hydrological cycle and each flow point: relation between transit time and TOC proposed by Batiot et al. (2003) allowed to connect transit time values to HIX. However, this relation was based on a very limited number of samples and had a high uncertainty.

In spite of these limitations, Blondel's study results were consistent and led to the identification of a clear link between HIX and transit time. Based on the critical analysis of these previous studies, we first analyzed water fluorescence on 289 water samples from 4 springs and 10 flow points located in the unsaturated zone of the Vaucluse karst system. 2D spectra of organic matter fluorescence were compared with Zsolnay emissions windows. Main organic matter fluorescent components in water samples were identified based on parallel factor analysis (PARAFAC) and bibliographical review. We then proposed a new humification index called Transit Time index (TTi) based on Ohno (2002) formula but using PARAFAC components of heavy and light organic matter compounds from our samples instead of 2D windows. Finally, we evaluated TTi relevance as a transit time tracer by: (i) performing a detailed analysis of its dynamic on a selected (Millet) spring and (ii) comparing its mean value over karst springs of Fontaine de Vaucluse system.

2. Materials and Methods

2.1 Study site

This study was carried out in the Vaucluse karst system (southeastern France) (Fig. 1). This hydrosystem mainly composed of outcropping Marine Cretaceous limestones is unusual in terms of dimension and volume. Its main outlet, Fontaine de Vaucluse spring, has a mean flow rate of 23,3 $m^3.s^{-1}$ (from 01/1877 to 06/2006 Cognard-Plancq et al., 2006) which is one of the highest in Europe. It is also characterized by a particularly thick unsaturated zone (~800 m). Monitoring of flows in its unsaturated zone at depths ranging from ~30 m to almost 500 m is made possible through the artificial galleries of the LSBB (https://lsbb.cnrs.fr). Several outlets of less importance are also located on the recharge area of The Vaucluse karst system, the mains being Millet, St Trinit and Nesque springs (Table 1).

Spring	Catchment area	Karstification	UZ thickness	Lithology	Land use
Millet	~ 2,5 km²	Complex karstification - anastomoses in saturated zone	Thick ~ 70 m	Cretaceous/ Barremian limestones (marine)	Forest, lavender cultivation

https://doi.org/10.5194/hess-2022-100
Preprint. Discussion started: 31 March 2022

St Trinit	~ 2 km²	High degree, large karstic conduit	Thin ~ 10 to 20 m	Cretaceous/Aptian limestones (marine)	Anthropic activities, organic farming, town
La Nesque	~ 1 km²	Low degree, conduits of centrimetrious scale at the outlet	Thin ~ 10 to 20 m	Marneous limestones, Oligocène (lake)	Lavender cultivation
Fontaine de Vaucluse	~ 1160 km²	Variable but high in average	Very thick ~ 800 m	Cretaceous limestones (marine)	Cultivations, cities, forests
LSBB	≤ 1 km²	Variable	35 à 518 m	Cretaceous limestones (marine)	Forest and cultivation

Table 1: Main characteristics of monitored flow points from Batiot, 2002; Blondel, 2008; Emblanch et al., 1998; Lastennet, 1994; Ollivier, 2020 and field observations.

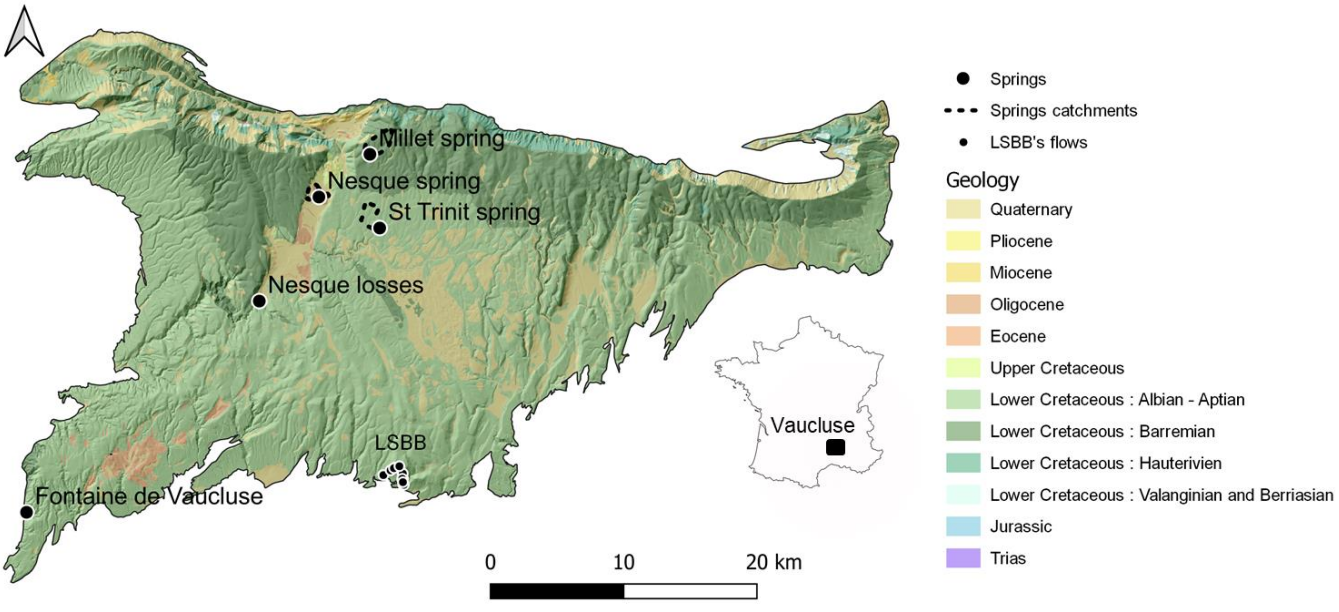

Figure 1: Location of monitored flow points on a 1:50000 geological map (BD-CHARM) from BRGM.

2.2 Sampling and fluorescence analysis methods

Bi-monthly sampling of all flow points was performed during a one-year monitoring (june 2020 to october 2021). Measurements of major elements, TOC, water stable isotopes were performed by UMR 1114 EMMAH respectively with ionic chromatography on DIONEX ICS1100, TOC Aurora 1030, and Picarro L2130-i. Excitation-emission matrix (EEM) and 2D spectra of organic matter fluorescence were performed at HydroSciences Montpellier using a spectrofluorometer SHIMADZU RF-5301 PC (xenon lamp). Wavelength windows for EEM were: λ_{ex}= [220 ; 450] nm, interval=10 nm ; λ_{em}= [250 ; 550] nm,

https://doi.org/10.5194/hess-2022-100
Preprint. Discussion started: 31 March 2022


Hydrology and Earth System Sciences
Discussions

interval=1 nm. Wavelengths for the 2D spectrum were λ_{ex}= 254 nm; λ_{em}= [220 ; 530] nm. The temperature was stabilized at 20°C in a bath with a thermostat. Slit-widths of 15 nm were used for the monochromators with a fast default scan speed. The stability of the apparatus was checked based on the Raman peak on fresh MilliQ water excited at 348 nm.

Identification of natural organic matter components in our samples was performed by both manual and automatic procedures. Manually peak picking was performed on raw EEM of over 10% of representative samples of the dataset, leading to the identification of about eighty fluorophores corresponding to seven different components. EEM were also treated thanks to R software and staRdom package (Pucher et al., 2019). Each of the 289 EEM was corrected with blank subtraction, Raman normalization (Lawaetz and Stedmon, 2009), and scattering removal (Lakowicz, 2006; Murphy et al., 2013). Removed scatter was interpolated with spline interpolation (Lee et al., 1997). PARAFAC modeling was then performed to extract organic matter components thanks to the same software and package using non-negative constraints for all modes.

2.3 Transit Time index (TTi) definition

Based on the fluorescence analysis of our samples we propose the Transit Time Index (TTi) which derives from the HIX definition of Ohno (2002) but differs by the analytic method of organic matter (2D vs 3D). TTi is thus the ratio of heavy organic matter (high emission wavelengths, humic-like organic matter) to heavy and light organic matter (low emission wavelengths, protein-like organic matter) Eq. (2):

$$TTi = \frac{\text{humic-like}}{(\text{humic-like})+(\text{protein-like})}, \quad (2)$$

where humic-like and protein-like parameters correspond to the sum of all compound weights of each type from the PARAFAC model. Unlike HIX, TTi considers the totality of groundwater fluorescent organic matter compounds. TTi value close to 1 means that organic matter is composed of low digestible organic matter (humic-like), which indicates relative long transit time. On the other hand, TTi close to 0 means that organic matter is composed of highly digestible organic matter (protein-like), which indicates very short transit time.

3 Results and discussion

3.1 Identification of organic matter compounds

3.1.1. 2D spectra results

The emission wavelengths of windows used to compute HIX have been compared to 2D spectra of natural fluorescence of representative samples from our dataset (Fig. 2). As compared to the proposed windows, i) the protein peak of Millet sample only partially fits inside, ii) the 370 nm protein-peak of St Trinit spring sample is shifted towards longer wavelengths. In both cases, emission of fluorescence of protein organic matter components is not correctly considered by HIX calculation. Proposed

https://doi.org/10.5194/hess-2022-100
Preprint. Discussion started: 31 March 2022

Hydrology and Earth System Sciences
Discussions

fluorescence windows are thus not appropriate to characterize organic matter in groundwater. We hypothesize that this mismatch may be related to the fact that groundwater's organic matter is older than that of its own source, which is the soil.

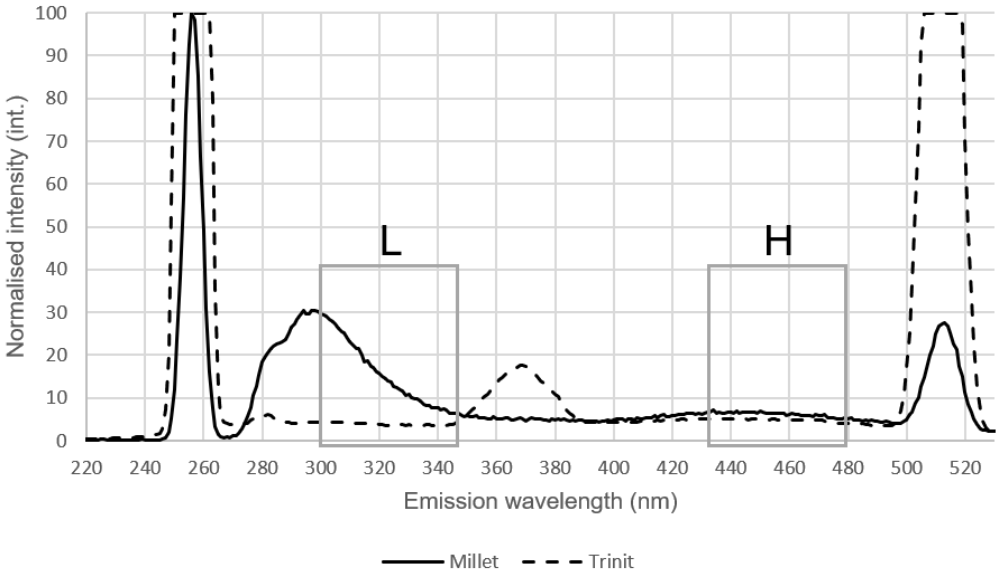

Figure 2: 2D spectra at excitation wavelength 254 nm for 2 representative samples (Millet 03/05/2021, St Trinit 01/02/2021). Comparison with Ohno (2002) H and L windows.

3.1.2 PARAFAC model results

The performed PARAFAC model managed with non-negative constraints contains 4 different components of organic matter. It was chosen for its explained variance of 0.9825, its core consistency of 92,7 % and it was checked thanks to split half analysis and Tucker's congruency, plotting of components and random initialization (Andersen and Bro, 2003). Three of the four identified components contain two close but distinguishable compounds (components 1, 2 and 4). PARAFAC components are in good agreement with manual peak picking performed on raw EEM, taken apart compound 3 which is affected by harmonics. Comparison with excitation-emission windows from the literature allows to identify organic matter compounds represented by each component (Fig. 3).

Component 1 is typical of heavy compounds belonging to humic-like organic matter type (Blondel, 2008; Quiers et al., 2014). **Component 2** is composed of two Tryptophan-like compounds. Indeed, compound with the longer excitation wavelength closely matches Trp 1 from Birdwell and Engel (2010) and compound with the shorter excitation wavelength appears to be another declination of Tryptophan-like organic matter, different from Trp 2 from Birdwell and Engel (2010). **Component 3** is consistent with P1 observation from Quiers et al. (2014). This compound lies close to Trp 2 but its emission wavelength is too high for it to belong to Tryptophan-like organic matter. Quite surprisingly it is far from P1 observation of Blondel (2008). We hypothesize that P1 was mistaken for Tryptophan-like organic matter by Blondel (2008). Component 3 also lies far from the hand peak picking window of P1, probably because hand-peak picking was performed on

https://doi.org/10.5194/hess-2022-100
Preprint. Discussion started: 31 March 2022

Hydrology and Earth System Sciences
Discussions

raw EEM not yet corrected from harmonics. **Component 4** contains one main compound which we assume to be Tyrosine-like organic matter because it lies really close to Tyr 1 observation of Mudarra et al. (2011). A second component with lower intensity may correspond to Tyr 2 of Mudarra et al. (2011).

The four components identified by PARAFAC modelling can thus be gathered into humic-like organic matter (component 1) and protein-like organic matter (components 2, 3 and 4). We also note that 2D spectra at 254 nm may accurately illustrate the maximum intensity of Trp2 and H2 but misses maximum intensity of H1. Use of EEM instead of 2D spectra thus appears necessary to achieve the characterization of all the humic-like and protein-like compounds required for humification index calculation.

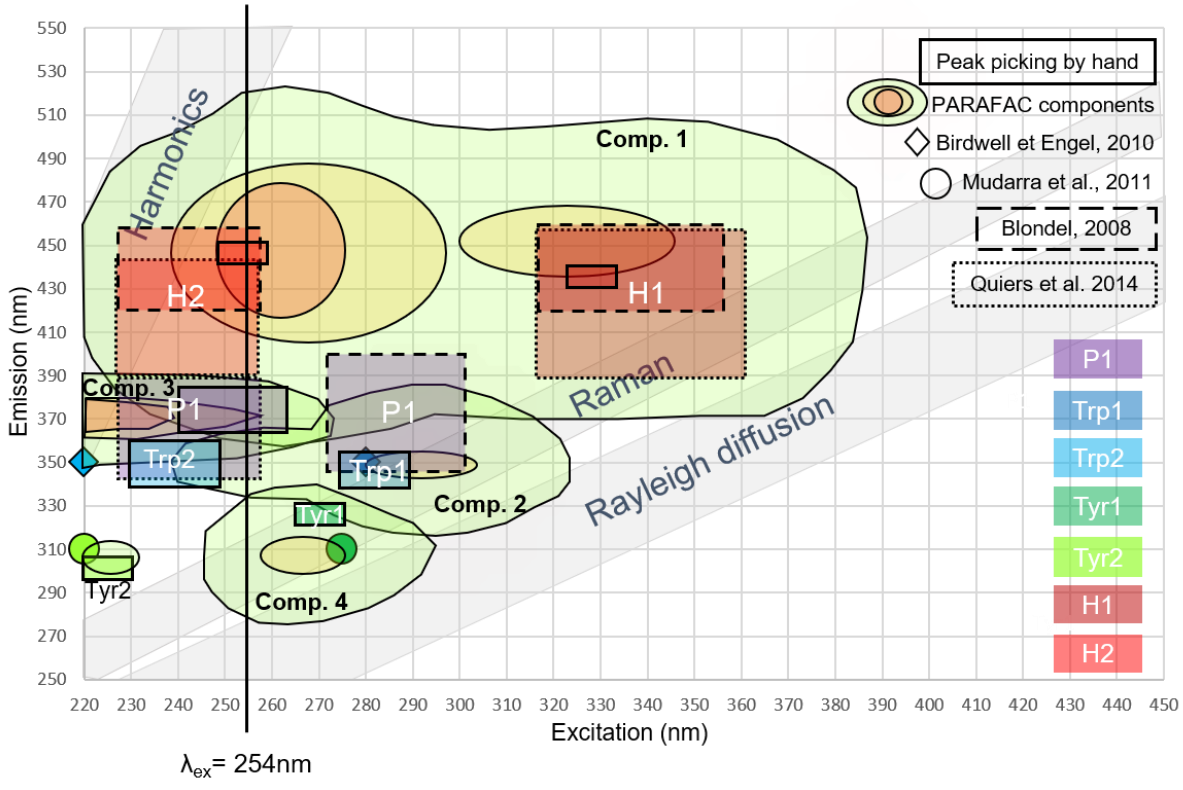

Figure 3: Comparison of organic matter components location in EEM matrix in literature and our study.

3.2 TTi application at Millet spring

3.2.1 Hydrodynamic and hydrochemical functioning of Millet spring

Descriptive statistics of major ions, TOC, electrical conductivity, humic-like and protein-like organic matter, TTi, standard deviation, and coefficient of variation are available in Table 2. Discharge at Millet spring reacts sharply to rainfall events (Fig. 4) which indicates that the karst network is mature. On the contrary, natural tracers such as $d^{18}O$ and major elements are not well correlated with discharge and have low amplitude variations highlighting the high mixing ability of the Millet system. It

https://doi.org/10.5194/hess-2022-100
Preprint. Discussion started: 31 March 2022


Hydrology and Earth System Sciences
Discussions

is particularly the case of $d^{18}O$ whose variations are close to detection limits. Such global hydrochemical stability suggests the presence of a saturated zone in which the mixing of waters is particularly effective, which we relate to the structure of its karstification (anastomose).

Electrical conductivity correlates well with discharge and highest conductivities are reached during high discharge with a 2 to 4 days delay, which is unusual for karsts systems except at the early stage of high water when infiltrated water flushes out old water (piston effect). This rise in electrical conductivity is mainly carried by Ca^{2+} and HCO_3^- contents. As $d^{18}O$ varies little, this rise cannot be attributed to recently infiltrated waters with high PCO_2 coming from soil. It thus reflects a relatively long interaction time with rocks and soil and thus a relatively long transit time or storage duration. Arrival of water associated with short residence time is usually also evidenced by TOC (Batiot et al., 2003). TOC is a natural tracer of fast infiltration, which increases with decreasing transit time. From a hydrodynamic point of view, Millet is a fast-reacting karstic system and TOC is thus expected to increase sharply during flood events. Measured TOC does correlate with discharge, but it varies little and doesn't exceed 2 $mg.L^{-1}$ showing evidence of a mix in the saturated zone. While proportion of fresh water during floods at Millet is thus too low to cause a decrease in electrical conductivity, TOC does provide evidence of arrival of water with short transit times, but limits of sensitivity of this tracer also seem to be reached.

Parameter	Unit	Min	Max	Mean value	SD	CoV (%)
TTi	-	0.11	0.93	0.41	0.19	46
Humic-like	intensity	0.05	3.97	1.17	0.09	8
Proteic-like	intensity	0.44	0.75	0.61	0.84	138
CE	$\mu S.cm^{-1}$	305.6	338.5	317.7	8.48	3
$d^{18}O$	‰	-8.96	-8.76	-8.89	0.05	-0.6
Mg^{2+}	$mg.L^{-1}$	0.74	1.51	1.06	0.20	19
SiO_2	$mg.L^{-1}$	5.45	7.62	7.00	0.53	8
TOC	$mg.L^{-1}$	0.82	2.15	1.03	0.24	23
Cl^-	$mg.L^{-1}$	1.38	2.38	1.86	0.28	15
NO_3^-	$mg.L^{-1}$	0.39	2.5	1.11	0.45	40
SO_4^{2-}	$mg.L^{-1}$	2.36	4.2	3.17	0.35	11

Table 2: Descriptive statistics of major ions, TOC, electrical conductivity, humic-like and protein-like organic matter, and TTi. SD standard deviation, CoV coefficient of variation, over the period june 2020 to october 2021.

https://doi.org/10.5194/hess-2022-100
Preprint. Discussion started: 31 March 2022

Figure 4: Millet spring time series of rain, discharge, TTi, humic-like (component 1) and protein-like (sum of components 2, 3 and 4) fluorescent organic matter, continuous & punctual electrical conductivity, delta O-18, magnesium, silica, chlorides, nitrates and sulfates contents over the period june 2020 to october 2021 period. Colors above the discharge plot and numbers on TTi curve correspond to Figure 6 (b).

3.2.2 Relation between TTi components and other variables

Correlation matrix presented in Figure 5 (a) shows a positive correlation between TTi and component 1, and anticorrelation with components 2, 3 and 4 which stems from TTi formula. The anticorrelation is stronger with Tyrosine due to its highest digestibility leading to a higher variability of its concentrations. Indeed, fluorescent organic matter digestibility decreases with increasing emission wavelength and Tyrosine has the lower (Fig. 3). Components 2 and 3 are strongly correlated, caused by the similarity of their emission wavelength and thus of their degradation kinetics. The highest correlation of the first (humic-like) component is found with electrical conductivity and discharge. Humic-like has the longest lifetime of all fluorescent

https://doi.org/10.5194/hess-2022-100
Preprint. Discussion started: 31 March 2022

Hydrology and Earth System Sciences
Discussions

organic matter because of its low digestibility and it thus has the highest emission wavelength (Fig. 3). Humic-like organic matter is thus always present in the system as seen in Figure 4 and thus may vary at the same low frequency as electrical conductivity and discharge while protein-like organic matter, because of their short life duration, may vary at high frequency. TTi correlation with magnesium was expected because this tracer has increasing values with transit time like TTi. But TTi is surprisingly anticorrelated with SiO_2. This anticorrelation is mainly carried by Tyrosine variation. Usually, rock dissolution is the main source of dissolved silica, inducing increasing contents with transit time. If so, SiO_2 would be correlated with TTi, magnesium and electrical conductivity. At Millet, SiO_2 is anticorrelated with these elements and correlated with Tyrosine, which has decreasing contents with increasing transit time, thus indicating similar SiO_2 and Tyrosine kinetics, both coming from an organic source (soil). This hypothesis is validated by the high content of SiO_2 in Millet soil water (around 10 $mg.L^{-1}$ in November 2000; Batiot, 2002).

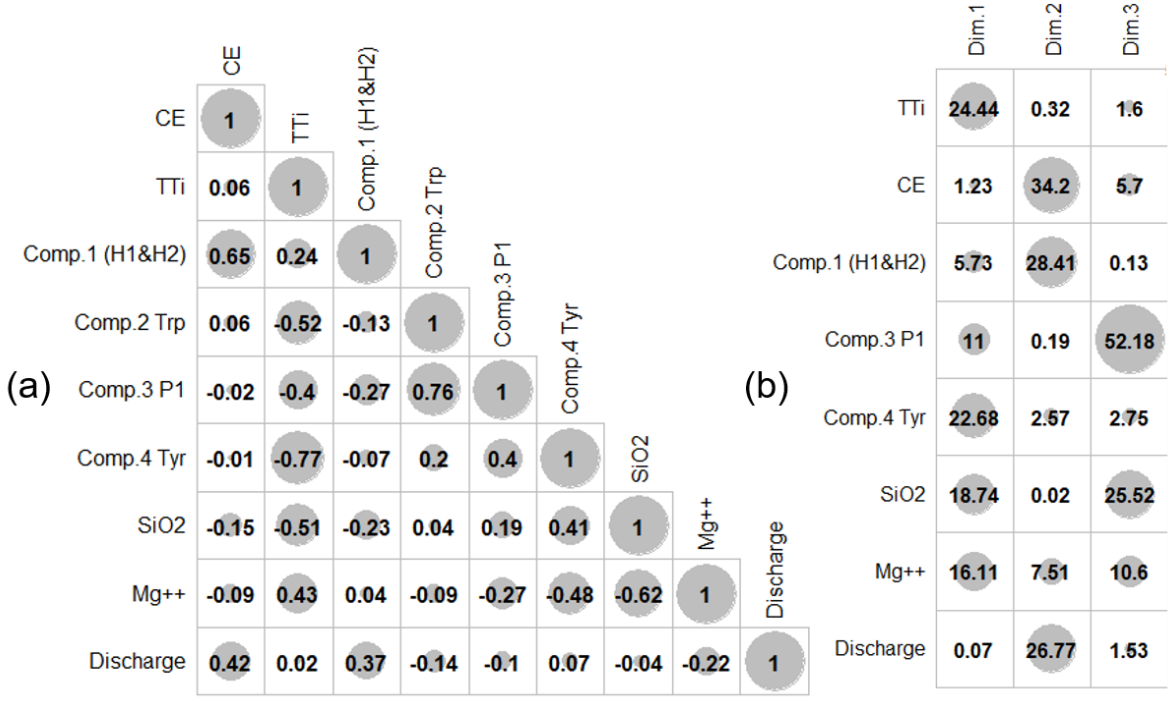

Figure 5: Correlation matrix of variables (a) and variables contributions to the three principal components of PCA (b).

PCA was performed on 27 Millet spring samples with TTi, TTi components (Tyr, P1, H1&H2) and other variables related to transit time (electrical conductivity, discharge, magnesium and silica contents). Component 2 Trp was omitted because of its strong correlation with P1 (0.94, Fig.5 (b)) and its lower intensity as seen is Figure 3. The 3 principal axes of PCA explain about 73,2 % of the total variance. The first principal component (Dim 1) represents 36.7 % of total variance, the second (Dim. 2) 25,2 % and the third (Dim. 3) 11,3 %. They are carried by different variables as seen in Figure 5 (b). PCA results are provided in Figure 6.

https://doi.org/10.5194/hess-2022-100
Preprint. Discussion started: 31 March 2022


Hydrology and Earth System Sciences
Discussions

The first dimension is negatively scored with Tyrosine and SiO_2 and positively with Mg^{++} and TTi. These variables have in common their high frequency variation. Indeed, Tyrosine has the shorter lifetime duration of tested variables and is linked to silica. Its degradation kinetics is therefore very short, implying strong variations over time. TTi and magnesium are in the opposite direction. For TTi, it is because of its opposition to protein-like organic matter compounds, caused by its construction. For magnesium, this opposition is caused by the dilution of stored water by freshwater supply. Dim. 1 thus corresponds to high frequency variations led by rain events (daily scale) bringing fresh organic matter rich in Tyrosine and SiO_2, and diluting stored water implying magnesium decrease.

The second dimension is positively scored with electrical conductivity, discharge and humic-like organic matter (component 1). These variables evolve at low frequency (monthly to seasonal scale) mainly due to the alternance of low/high flow periods. It can be surprising that humic-like organic matter evolves in the same direction than electrical conductivity and discharge, but as TOC, humic-like shows a mix of stored and fresh water, with enough fresh water to see a slight humic-like increase, but not enough to induce a major electrical conductivity decrease. This dimension seems to indicate a seasonal variation of humic-like organic matter, implying a seasonal variation of TTi.

The third dimension is negatively scored with SiO_2 and positively with P1 and magnesium. In comparison with other variables, these two variables have intermediary frequency variations. Indeed, P1 emission wavelength is between the emission wavelengths of humic-like and Tyrosine (Fig. 3) and thus has an intermediate lifetime duration (from weeks to months). Magnesium is little explained by Dim. 3 (10,6 %) but it is still positively scored with it, suggesting an organic source of magnesium (soil). SiO_2 is in the opposite direction which shows a part of its content coming from rock dissolution or mineralisation.

Variation frequency can easily be linked with transit time because natural tracers of a precise range, must, by definition, vary in this range. Dim. 1 is thus susceptible to trace short transit time at daily scale, Dim. 2 long transit time at monthly/seasonal scale, and Dim. 3 intermediate transit time at weekly scale.

Projection of samples on the factor-plane is consistent with the different ranges of transit time associated with PCA dimensions (Fig. 6 (b) and (d)). Samples from the **2020 low-water period** are mainly expressed by Dim. 2 and Dim. 3 corresponding to intermediate to low variation frequency. It is consistent because during low-flow periods, expected transit time is long and may correspond to months. These samples are also, to a lesser extent, expressed by Dim. 1. For example sample 5 has the lowest Dim. 1 score and corresponds to the reaction to a rain whereas sample 7 which has the higher score, corresponds to a dry period during the low flow period.

The **2021 low-water period** has more frequent rainfall events. As compared to the 2020 low-water period, spread of samples from the 2021 low-water period is higher on factor planes 1 and 3. Samples from this period are mainly explained by Dim 1 and 3 corresponding to intermediate and short transit time in agreement with Millet's well karstified system inducing fast reactions. **Flood event** samples are expressed by Dim. 1 and Dim. 2 - high and low variations frequency. Samples close to Dim. 2 reflect the flush out of stored water (piston effect - samples 12, 16 and 20), they correspond to the beginning of floods.

https://doi.org/10.5194/hess-2022-100
Preprint. Discussion started: 31 March 2022


Hydrology and Earth System Sciences
Discussions

Sample 1 is aligned with Dim. 1. It corresponds to freshwater arrival at the end of a flood, thus with short transit time (see time series Fig. 4).

Short low-water period samples appear in no particular dimension because water age after a flood event may differ depending on intensity of previous floods, piston effect duration, and also contain very recent water as seen in the case of the long-duration, 2021 rainy low water period.

Observation of sample projection on PCA results thus validate the accuracy of the identified dimensions, and the viability of TTi components to illustrate different ranges of transit time at Millet karstic system. TTi is therefore able to provide more information about the functioning of complex karstic systems, even in highly mixing systems like Millet.

3.2.3 Time variability of Transit Time index (TTi)

Lowest TTi values occur in low flow periods: TTi is 0.3 in average during 2021 low flow period and 0.5 in average during the 2020 low flow period (Fig. 4). It is consistent with the relative transit times expected over these two periods based on magnesium contents (~1.3 in 2020 vs ~0.8 $mg.L^{-1}$ in 2021) and hydrometeorological conditions as rainfall is more uniformly distributed in time in the 2021 low-flow period than in the 2020.

TTi behavior during flood period is complex as it may correlate either (i) negatively (ex. samples 12, 15) or (ii) positively (ex. samples 8-9, 20) with discharge. Case (i) is expected when infiltrated fresh water, which is rich in organic matter (protein-like compounds), are dominant and thus yielding a decrease in TTi. Case (ii) is unusual except at the early stage of high water when infiltrated water flushes out old water (piston effect). At later stages it may be related to stored to fresh water ratio too high to induce a decrease in TTi for example in the case of short floods.

It thus appears that TTi is able to identify piston effect and also, as TOC, to identify a slight proportion of freshwater in a mix. However, TTi is more sensitive as seen by its punctual correlation with discharge (case (ii)) and its punctual uncorrelation with TOC as in samples 5 to 8 and 14 to 17 (Fig. 4).

Analysis of time variability of TTi at Millet spring thus (i) reinforces the consistency of TTi variations, (ii) indicates a better sensitivity of this marker than TOC to freshwater arrivals. Thanks to its higher sensitivity, TTi also allows a better understanding of the Millet karstic system where other natural tracers fail.

https://doi.org/10.5194/hess-2022-100
Preprint. Discussion started: 31 March 2022

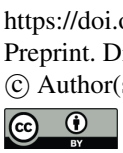

Hydrology and Earth System Sciences
Discussions

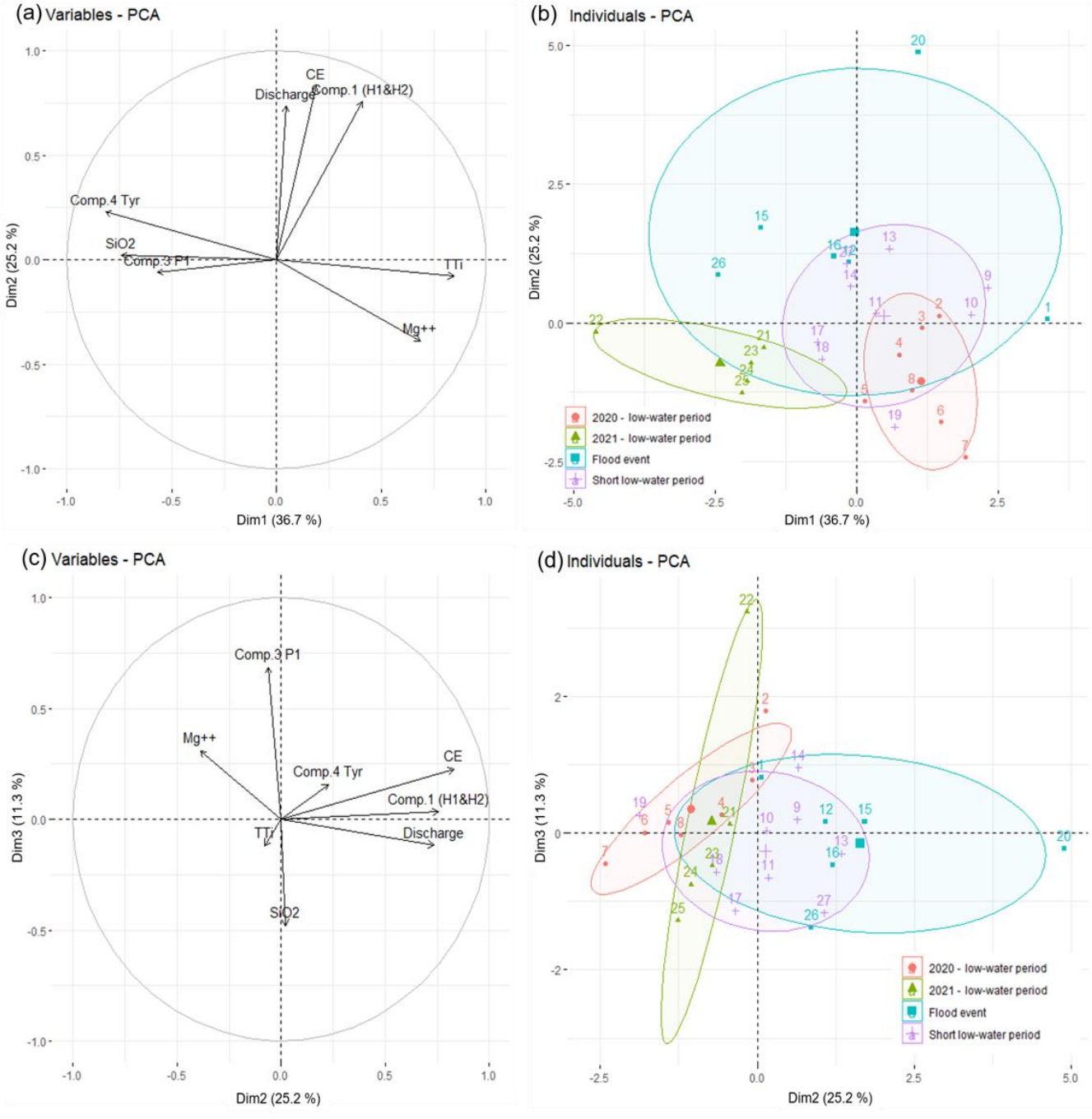

Figure 6: PCA performed with Millet spring samples thanks to the following variables: TTi components, TTi, SiO_2, Mg^{2+}, electrical conductivity, discharge. Dimensions 1 and 2 presented in (a) and (b), dimensions 2 and 3 in (c) and (d). (a) and (c) Variables: interpretation of transit time poles; (b) and (d) Individuals: Point color corresponding to hydrodynamic periods (see Figure 4), point label to sample number (see Figure 4), confidence ellipse 70%.

https://doi.org/10.5194/hess-2022-100
Preprint. Discussion started: 31 March 2022


Hydrology and Earth System Sciences
Discussions

3.3 Comparison of average TTi values of Vaucluse karst springs

Visual comparison of electrical conductivity, chloride, magnesium, nitrates, TOC and TTi distributions from our dataset is provided in Figure 7. TTi variability is higher than that of other elements on each monitored spring which suggests that TTi is more sensitive. TTi median value increases from St Trinit to Nesque springs via Millet.

Spring with lowest TTi values (St Trinit) has the highest karstification level, thinnest unsaturated zone, highest nitrates and chloride contents which is compatible with shorter median transit times. As compared to St Trinit, Millet has lower and less variable chlorides and nitrates contents, and less variable TOC. Anastomose karst network in its saturated zone is assumed to provide a mixing effect of infiltrated water. We thus suppose that this system is little affected by fast infiltration. Highest TTi values are found at the Nesque spring, which is the less karstified system. Relative distribution of TTi values at St Trinit, Millet and Nesque springs are therefore consistent with the expected behavior of a transit time indicator, depending on their karstification type and thus on their hydrodynamical and hydrochemical responses. Median value of TTi at Fontaine de Vaucluse spring is similar to that of Nesque spring. However, mean water transit time at Fontaine de Vaucluse spring is expected to be significantly higher than that of Nesque spring because it is the outlet of a wider system with thicker saturated and unsaturated zones. This inconsistency is related to the relatively short time scale of transit times covered by TTi. Maturation of organic matter components constituting TTi is almost complete after 6 months (TOC degradation; Batiot, 2002) while the water flowing from the Fontaine de Vaucluse spring is a mixture of water with a long residence time (several years) and freshwater coming from rapid infiltrations through the shortcuts existing in the underground infiltration network (Margrita et al., 1970).Transit times of most Fontaine de Vaucluse samples are thus probably out of the range of relevance of TTi to quantitatively identify transit time values. However, TTi as it is more sensitive may identify freshwater arrivals in the mix of waters flowing at the Fontaine de Vaucluse spring during flood events.

https://doi.org/10.5194/hess-2022-100
Preprint. Discussion started: 31 March 2022

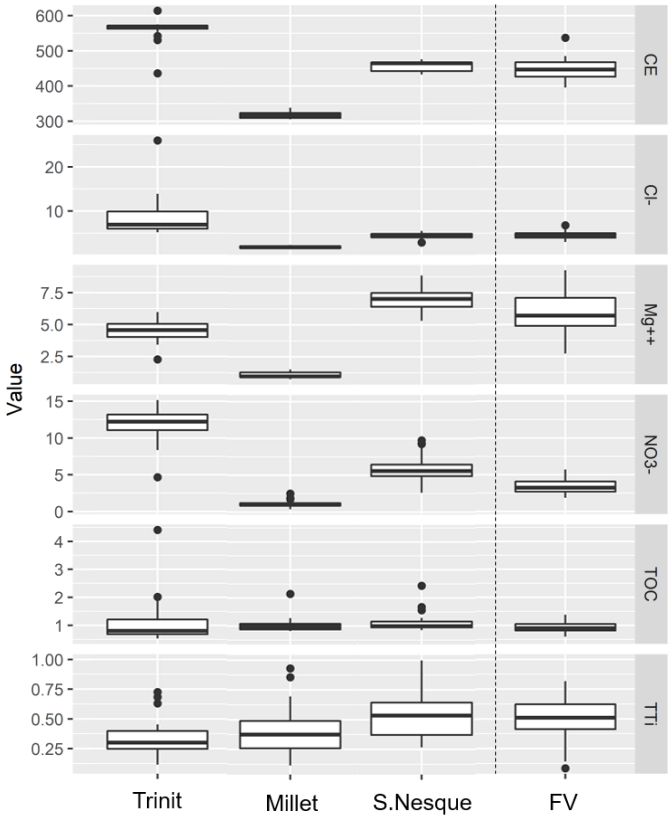

Figure 7: Boxplots of electrical conductivity, chlorides, magnesium, nitrates, TOC and TTi of Fontaine de Vaucluse (FV, 25 samples), Millet (27 samples), Nesque (S.Nesque, 29 samples) and St Trinit (Trinit, 29 samples) springs.

Conclusion

Water transit time can be estimated thanks to natural tracers but few of them are usable in the 0-6 months range. The main purpose of this work was to analyze the potential of the ratio of heavy to light-weight organic compounds (HIX) as a natural tracer of short transit time in karst systems with a strong fast infiltration component in order to characterize the vulnerability of the aquifer.

Critical analysis of former studies showed that although the link between HIX and transit time seems consistent, the whole methodological approach needed to be consolidated. Natural fluorescence from 289 water samples from 4 springs and 10 flow points located in the unsaturated zone of the Vaucluse karst system was characterized by parallel factor analysis (PARAFAC) of the EEM, thus (i) allowing the identification of main fluorescent compounds of sampled groundwater, and (ii) evidencing the inadequacy of HIX emission windows to characterize groundwater organic matter. We then proposed a new humification

https://doi.org/10.5194/hess-2022-100
Preprint. Discussion started: 31 March 2022


Hydrology and Earth System Sciences
Discussions

index called Transit Time index (TTi) based on Ohno (2002) formula but using 3D PARAFAC components of heavy and light organic matter instead of 2D windows.

Finally, we evaluated TTi relevance as a potential transit time tracer by: (i) performing a detailed analysis of its dynamics on a selected spring (Millet spring) and (ii) comparing its mean value over karst springs of Fontaine de Vaucluse system. Principal component analysis (PCA) of TTi, TTi components and other hydrochemical parameters monitored at Millet put in relief the time scales of variability associated with the different organic matter compounds, which we relate to their digestibility. PCA results also provided evidence that TTi can detect a small proportion of fast infiltration water within a mix, while other natural tracers of transit time provide no or less sensitive information. Relative distribution of TTi at monitored karst springs is also consistent with relative transit times expected for small-scale, short average transit times systems.

It thus appears that TTi has the potential to become a transit time tracer in the 0-6 months range where existing tracers fail, in the case of water with transit times in this range and not impacted by water that is too old. Otherwise, TTi, as it is more sensitive, may still identify freshwater arrivals in mixtures.

TTi potential should be confirmed by an in-depth analysis of TTi behavior and its possible seasonal variations on other karst systems. As information on transit times provided by TTi is only qualitative at this stage, laboratory or field-controlled experiments will be required to assess the degradation kinetics of these organic materials in the natural environment.

Acknowledgments

This work was performed within the framework of the FDV/LSBB observation site, which is part of OZCAR (French network of Critical Zone observatories), SNO KARST (French observatory network, www.sokarst.org) initiative of INSU/CNRS which seeks to support knowledge sharing and promote cross-disciplinary research on karst systems, and of the H+ observatory network.

The authors would like to express their gratitude to the LSBB team for their technical and logistic help. A special acknowledgement to SIAEPA from the Sault region and Veolia for giving us access to Nesque spring.

Financial support of the ALBION research project initiated by TotalEnergies S.A. is gratefully acknowledged. Authors also express their gratitude to the doctoral school GAIA (N°584) for financial support through a doctoral scholarship.

References

Andersen, C.M., Bro, R.: Practical aspects of PARAFAC modeling of fluorescence excitation-emission data, J. Chemom. 17, 200–215, https://doi.org/10.1002/cem.790, 2003.

Batiot, C.: Etude expérimentale du cycle du carbone en régions karstiques: apport du carbone organique et du carbone minéral à la connaissance hydrogéologique des systèmes, Ph.D. thesis, Université d'Avignon et des Pays de Vaucluse, France, 2002.

Batiot, C., Liñán, C., Andreo, B., Emblanch, C., Carrasco, F., Blavoux, B.: Use of Total Organic Carbon (TOC) as tracer of diffuse infiltration in a dolomitic karstic system: The Nerja Cave (Andalusia, southern Spain), Geophys. Res. Lett. 30, https://doi.org/10.1029/2003GL018546, 2003.

Birdwell, J.E., Engel, A.S.: Characterization of dissolved organic matter in cave and spring waters using UV–Vis absorbance and fluorescence spectroscopy, Org. Geochem. 41, 270–280, https://doi.org/10.1016/j.orggeochem.2009.11.002, 2010.

Blondel, T.: Expérimentation et application sur les sites du Laboratoire Souterrain à Bas Bruit (LSBB) de Rustrel – Pays d'Apt et de Fontaine de Vaucluse, Ph.D. thesis, Université d'Avignon et des Pays de Vaucluse, 2008.

Blondel, T., Emblanch, C., Batiot-Guilhe, C., Dudal, Y., Boyer, D.: Punctual and continuous estimation of transit time from dissolved organic matter fluorescence properties in karst aquifers, application to groundwaters of 'Fontaine de Vaucluse' experimental basin (SE France), Environ. Earth Sci. 65, 2299–2309, https://doi.org/10.1007/s12665-012-1562-x, 2012.

Cognard-Plancq, A.-L., Gevaudan, C., Emblanch, C.: Historical monthly rainfall- runoff database on Fontaine de Vaucluse karst system: a review and lessons, 2006.

Emblanch, C., Blavoux, B., Puig, J.M., Couren, M.: Le marquage de la zone non saturée du karst à l'aide du Carbone 13: The use of carbon 13 as a tracer of the karst unsaturated zone, Comptes-Rendus Séances Académie Sci. Séries IIA-Earth and Planetary Science, 327–332, 1998.

Ewald, M., Berger, P., Visser, S.A.: UV-visible absorption and fluorescence properties of fulvic acids of microbial origin as functions of their molecular weights, Geoderma 43, 11–20, https://doi.org/10.1016/0016-7061(88)90051-1, 1988.

Lakowicz, J.R.: Principles of fluorescence spectroscopy, 3rd ed. ed. Springer, New York, 2006.

Lapworth, D.J., Gooddy, D.C., Butcher, A.S., Morris, B.L.: Tracing groundwater flow and sources of organic carbon in sandstone aquifers using fluorescence properties of dissolved organic matter (DOM), Appl. Geochem. 23, 3384–3390, https://doi.org/10.1016/j.apgeochem.2008.07.011, 2008.

Lastennet, R.: Rôle de la zone non saturée dans le fonctionnement des aquifères karstiques: approche par l'étude physico-chimique et isotopique du signal d'entrée et des exutoires du massif du Ventoux (Vaucluse), Ph.D. thesis, Université d'Avignon et des Pays du Vaucluse, Avignon, France, 1994.

Lawaetz, A.J., Stedmon, C.A.: Fluorescence Intensity Calibration Using the Raman Scatter Peak of Water, Appl. Spectrosc, 63, 936–940, https://doi.org/10.1366/000370209788964548, 2009.

Lee, S., Wolberg, G., Shin, S.Y.: Scattered data interpolation with multilevel B-splines, IEEE Trans. Vis. Comput. Graph. 3, 228–244, https://doi.org/10.1109/2945.620490, 1997.

Margrita, R., Evin, J., Flandrin, J., & Paloc, H.: Contribution des mesures isotopiques à l'étude de la Fontaine de Vaucluse, *AIEA (Vienna) SM*, *129*(20), 333-348, 1970.

Malík, P., Švasta, J., Michalko, J., Gregor, M.: Indicative mean transit time estimation from δ18O values as groundwater vulnerability indicator in karst-fissure aquifers, Environ. Earth Sci. 75, 988, https://doi.org/10.1007/s12665-016-5791-2, 2016.

Mobed, J.J., Hemmingsen, S.L., Autry, J.L., McGown, L.B.: Fluorescence Characterization of IHSS Humic Substances: Total Luminescence Spectra with Absorbance Correction, Environ. Sci. Technol. 30, 3061–3065, https://doi.org/10.1021/es960132l, 1996.

https://doi.org/10.5194/hess-2022-100
Preprint. Discussion started: 31 March 2022


Hydrology and Earth System Sciences
Discussions

Mudarra, M., Andreo, B., Baker, A.: Characterisation of dissolved organic matter in karst spring waters using intrinsic fluorescence: Relationship with infiltration processes, Sci. Total Environ. 409, 3448–3462, https://doi.org/10.1016/j.scitotenv.2011.05.026, 2011.

Murphy, K.R., Stedmon, C.A., Graeber, D., Bro, R.: Fluorescence spectroscopy and multi-way techniques. PARAFAC, Anal. Methods 5, 6557, https://doi.org/10.1039/c3ay41160e, 2013.

Musgrove, M., Solder, J.E., Opsahl, S.P., Wilson, J.T.: Timescales of water-quality change in a karst aquifer, south-central Texas, J. Hydrol. X 4, 100041, https://doi.org/10.1016/j.hydroa.2019.100041, 2019.

Ohno, T.: Fluorescence Inner-Filtering Correction for Determining the Humification Index of Dissolved Organic Matter, Environ. Sci. Technol. 36, 742–746, https://doi.org/10.1021/es0155276, 2002.

Ollivier, C.: Caractérisation et spatialisation de la recharge des hydrosystèmes karstiques: Application à l'aquifère de Fontaine de Vaucluse, France, Ph.D. thesis, Université d'Avignon, 2020.

Pérotin, L., de Montety, V., Ladouche, B., Bailly-Comte, V., Labasque, T., Vergnaud, V., Muller, R., Champollion, C., Tweed, S., Seidel, J.-L.: Transfer of dissolved gases through a thick karstic vadose zone – Implications for recharge characterisation and groundwater age dating in karstic aquifers, J. Hydrol. 601, 126576, https://doi.org/10.1016/j.jhydrol.2021.126576, 2021.

Pronk, M., Goldscheider, N., Zopfi, J.: Microbial communities in karst groundwater and their potential use for biomonitoring, Hydrogeol. J. 17, 37–48, https://doi.org/10.1007/s10040-008-0350-x, 2009.

Pucher, M., Wünsch, U., Weigelhofer, G., Murphy, K., Hein, T., Graeber, D.: staRdom: Versatile Software for Analyzing Spectroscopic Data of Dissolved Organic Matter in R, Water 11, 2366, https://doi.org/10.3390/w11112366, 2019.

Quiers, M., Batiot-Guilhe, C., Bicalho, C.C., Perrette, Y., Seidel, J.-L., Van Exter, S.: Characterisation of rapid infiltration flows and vulnerability in a karst aquifer using a decomposed fluorescence signal of dissolved organic matter, Environ. Earth Sci. 71, 553–561, https://doi.org/10.1007/s12665-013-2731-2, 2014.

Sorensen, J.P.R., Carr, A.F., Nayebare, J., Diongue, D.M.L., Pouye, A., Roffo, R., Gwengweya, G., Ward, J.S.T., Kanoti, J., Okotto-Okotto, J., van der Marel, L., Ciric, L., Faye, S.C., Gaye, C.B., Goodall, T., Kulabako, R., Lapworth, D.J., MacDonald, A.M., Monjerezi, M., Olago, D., Owor, M., Read, D.S., Taylor, R.G.: Tryptophan-like and humic-like fluorophores are extracellular in groundwater: implications as real-time faecal indicators, Sci. Rep. 10, 15379, https://doi.org/10.1038/s41598-020-72258-2, 2020.

Stevanović, Z.: Karst waters in potable water supply: a global scale overview, Environ. Earth Sci. 78, 662, https://doi.org/10.1007/s12665-019-8670-9, 2019.

Tucker, S.A., Amszi, V.L., Acree, W.E.: Primary and secondary inner filtering. Effect of $K_2Cr_2O_7$ on fluorescence emission intensities of quinine sulfate, J. Chem. Educ. 69, A8, 1992.

White, W.B.: Karst hydrology: recent developments and open questions, Eng. Geol. 65, 85–105, https://doi.org/10.1016/S0013-7952(01)00116-8, 2002.

Zhang, Z., Chen, X., Li, S., Yue, F., Cheng, Q., Peng, T., Soulsby, C.: Linking nitrate dynamics to water age in underground conduit flows in a karst catchment, J. Hydrol. 596, 125699, https://doi.org/10.1016/j.jhydrol.2020.125699, 2021

Zsolnay, A., Baigar, E., Jimenez, M., Steinweg, B., Saccomandi, F.: Differentiating with fluorescence spectroscopy the sources of dissolved organic matter in soils subjected to drying, Chemosphere 38, 45–50, https://doi.org/10.1016/S0045-6535(98)00166-0, 1999.

https://doi.org/10.5194/hess-2022-100
Preprint. Discussion started: 31 March 2022


Hydrology and Earth System Sciences
Discussions

Author contribution: Matthieu Blanc and the SMBS (www.laSorgue.com) took water samples that were analyzed for major elements, TOC and water stable isotopes by Milanka Babic, Julien Dupont, Roland Simler and for fluorescence of organic matter by Leïla Serène. Formal data analysis was performed by Leïla Serène and Naomi Mazzilli. Christelle Batiot-Guilhe, Christophe Emblanch, Naomi Mazzilli and Leïla Serène provided critical feedback and helped to shape the research and the analysis. Gérard Massonnat acquired the fundings. Leïla Serène prepared the manuscript with contributions from all co-authors.

Competing interests. The authors declare that they have no conflict of interest.